Supporting Information

for

Unraveling Surface Polarization in Hydrothermally Derived $AgFeO_2$ Nanosheets for Enhanced Photoelectrochemical Performance

Shui-Miao Yu,[#] Xu-Dong Dong,[#] Zong-Yan Zhao[*]

Faculty of Materials Science and Engineering, Kunming University of Science and Technology, Kunming 650093, P. R. China

[#] These authors have equal contributions.

[*] Corresponding author, e-mail: zzy@kust.edu.cn

$$Ag^{+} + H_2O \rightarrow [AgOH_2]^{+} \rightarrow AgOH + H^{+} \rightarrow Ag_2O \qquad \text{(Eqs. 1)}$$

$$Ag_2O + 3\ H_2O \rightarrow 2\ [Ag(OH)_2]^{-} + 2\ H^{+} \qquad \text{(Eqs. 2)}$$

$$Fe^{3+} + 6\ H_2O \rightarrow [Fe(OH_2)_6]^{3+} \rightarrow [Fe(OH)_6]^{3-} + 6\ H^{+} \qquad \text{(Eqs. 3)}$$

$$[Ag(OH)_2]^{-} + [Fe(OH)_6]^{3-} + 4\ H^{+} \rightarrow AgFeO_2 + 6\ H_2O \qquad \text{(Eqs. 4)}$$

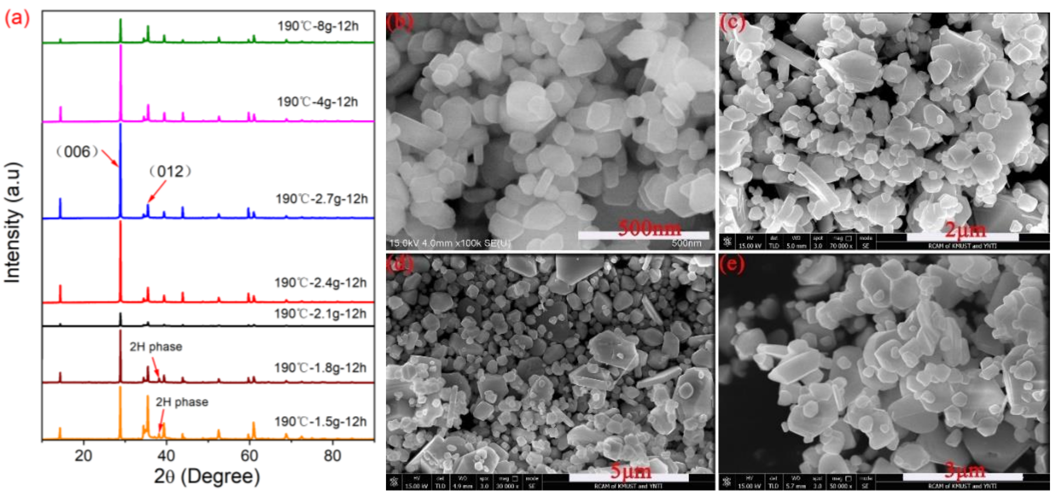

Figure S1. (a) XRD patterns; (b-e) SEM images of $AgFeO_2$ nanosheets with different NaOH additions at 2.1, 2.7, 4.0 and 8.0 g, respectively.

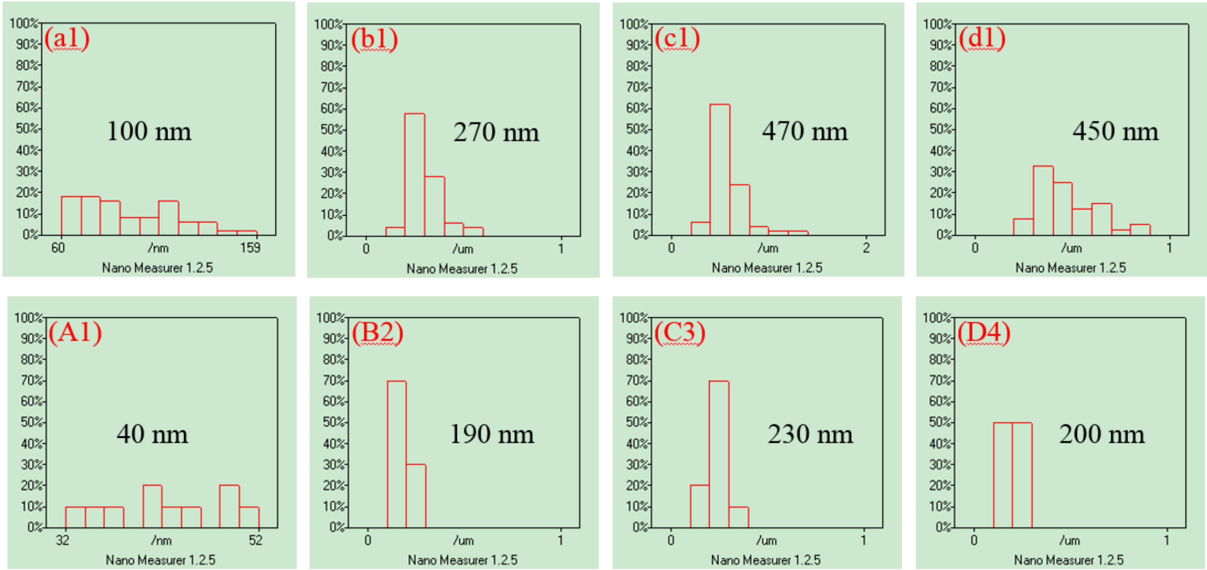

Figure S2. Influence of different NaOH concentrations on the width (A1-D1) and thickness (A1-D4) of $AgFeO_2$ nanosheets.

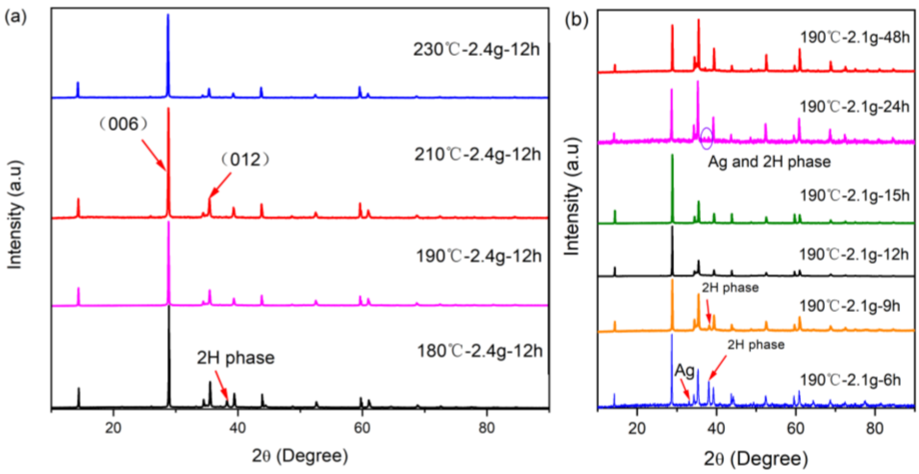

Figure S3. XRD patterns of $AgFeO_2$ nanosheets under (a) different reaction temperatures and (b) reaction time.

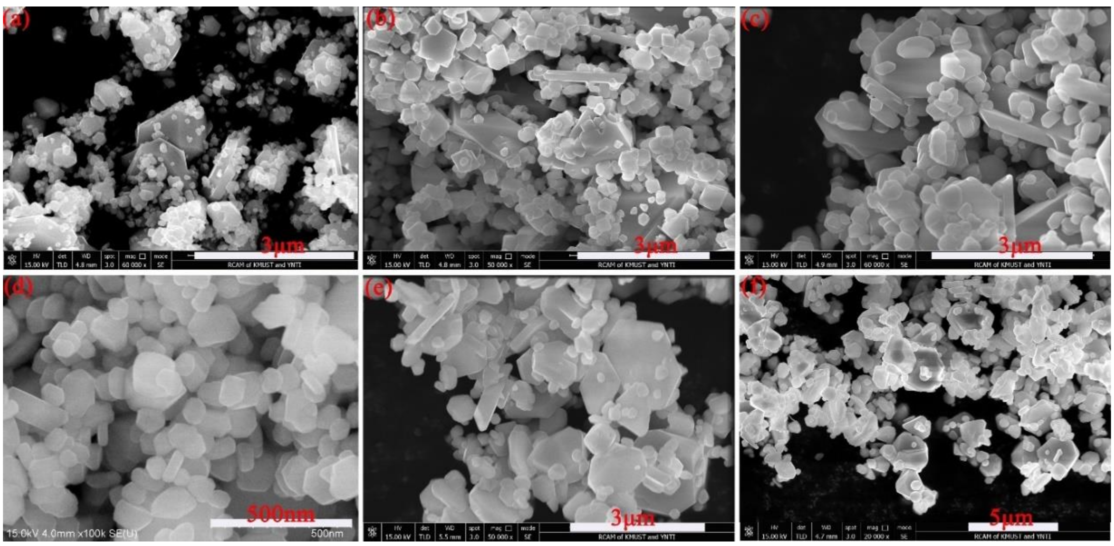

Figure S4. SEM images of $AgFeO_2$ nanosheet sizes regulated by different (a-c) reaction temperatures at 190, 210 and 230℃; (d-f) reaction time for 12, 15 and 24 h.

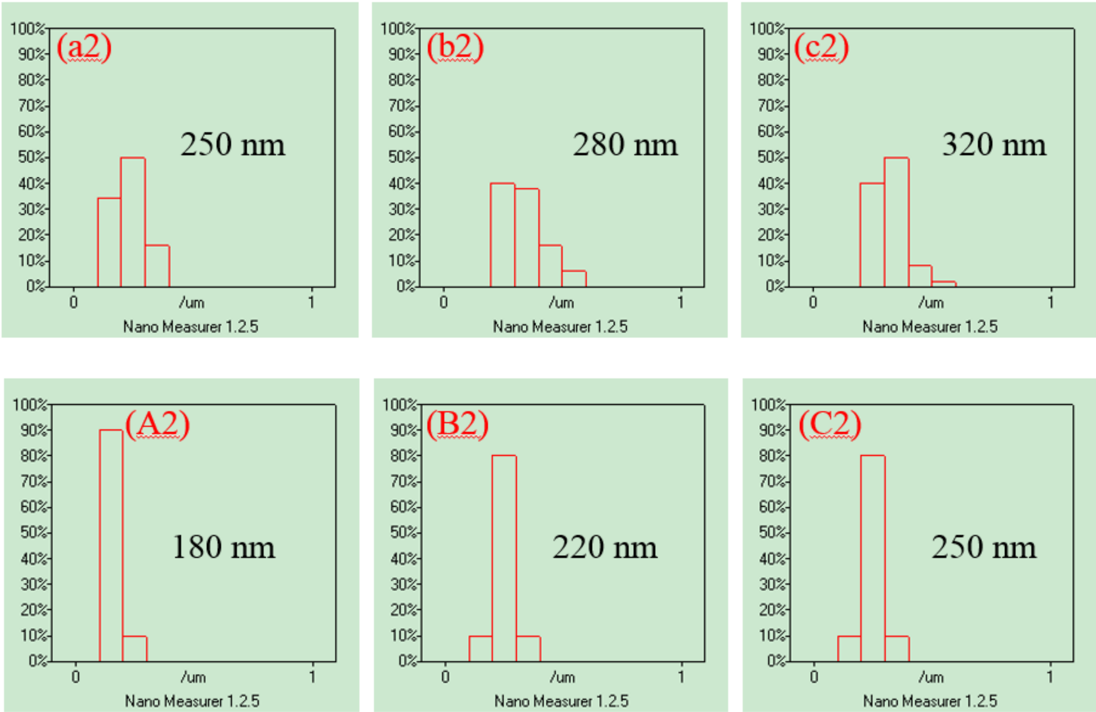

Figure S5. Effects of different reaction temperatures on the width (a2-c2) and thickness (A2-C2) of $AgFeO_2$ nanosheets.

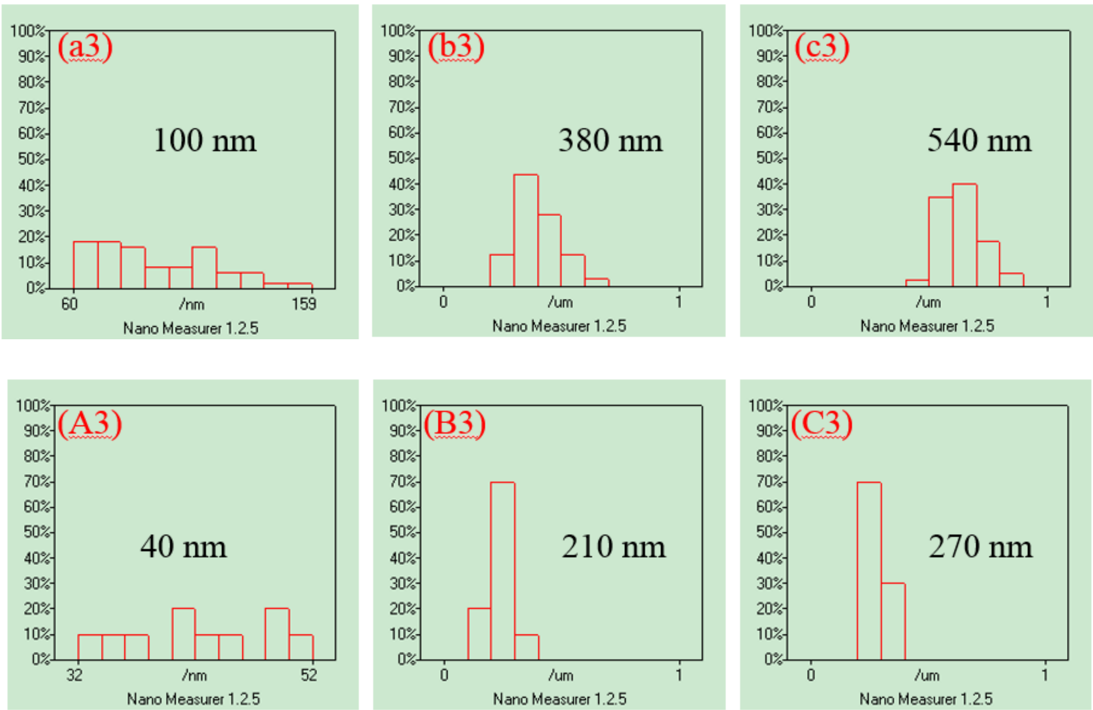

Figure S6. Effects of different reaction times on the width (a3-c3) and thickness (A3-C3) of $AgFeO_2$ nanosheets.

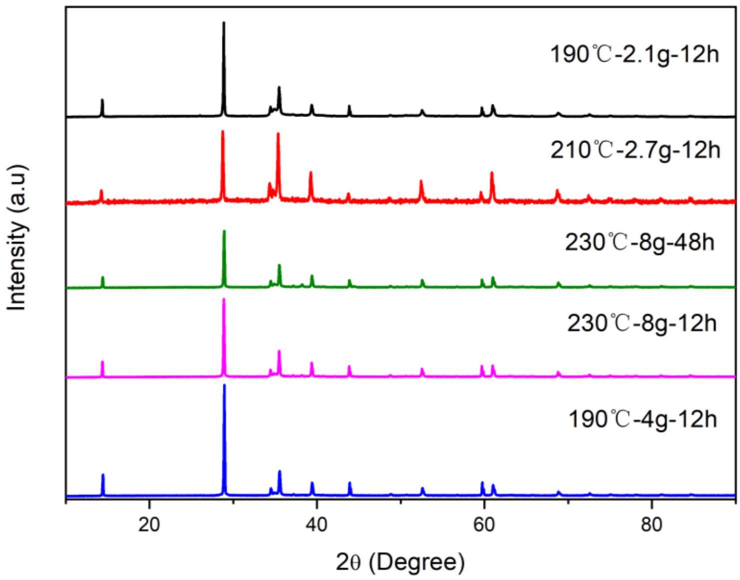

Figure S7. XRD pattern of $AgFeO_2$ nanosheets with different thickness.

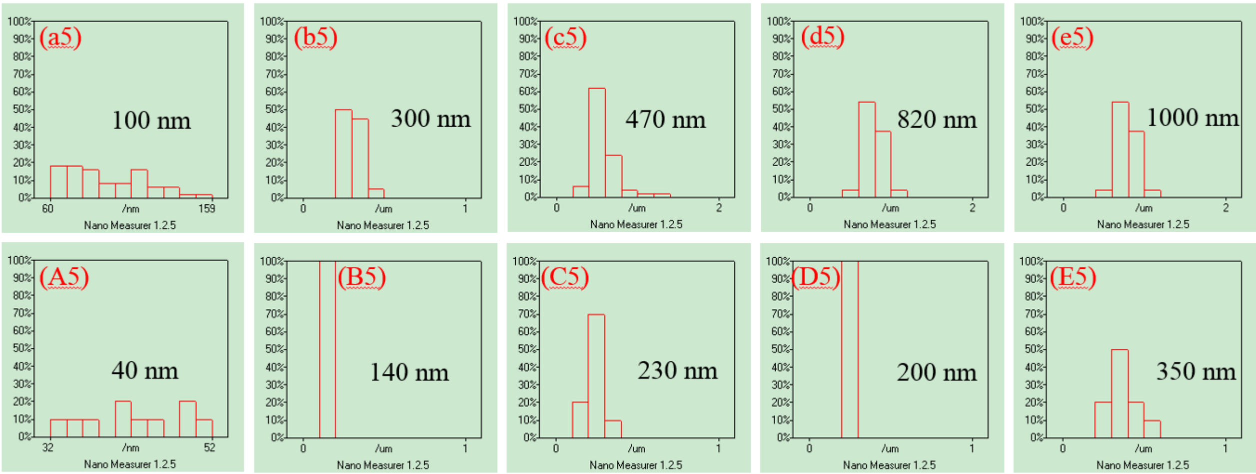

Figure S8. (a5-e5) width and (A5-E5) thickness of $AgFeO_2$ nanosheets with different thicknesses.

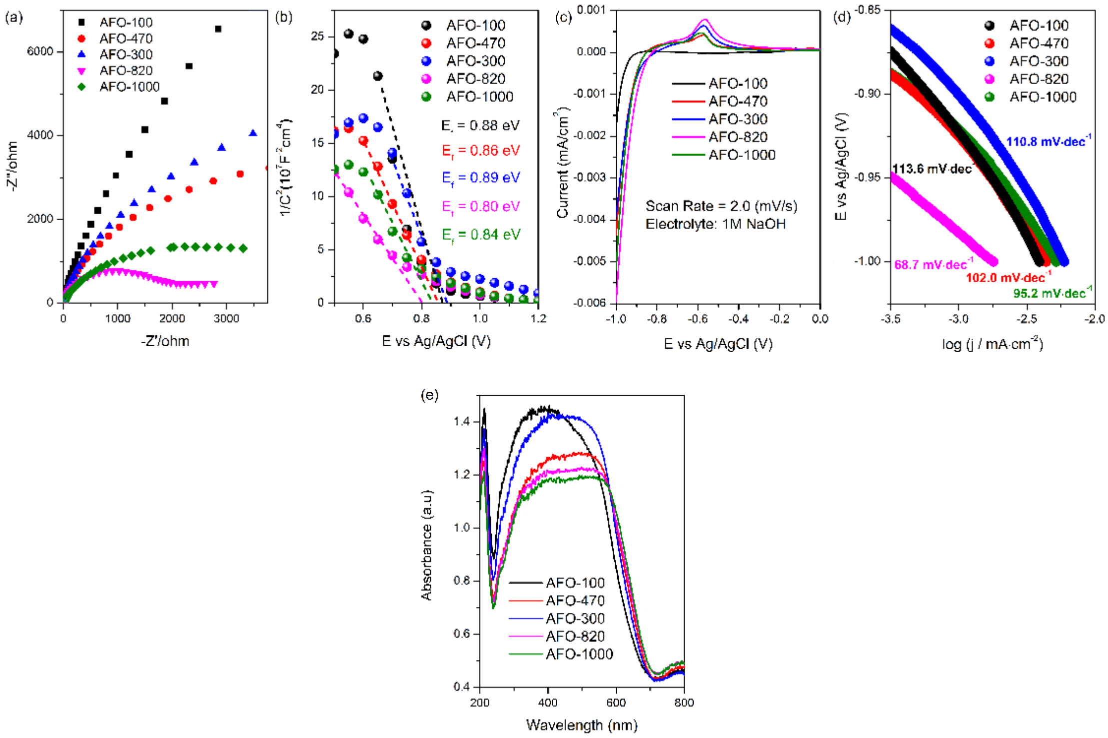

Figure S9. (a) EIS curve; (b) M-S curve; (c) LSV curve; (d) Tafel slope diagram; (e) UV-VIS curve of $AgFeO_2$ electrodes with different thickness.

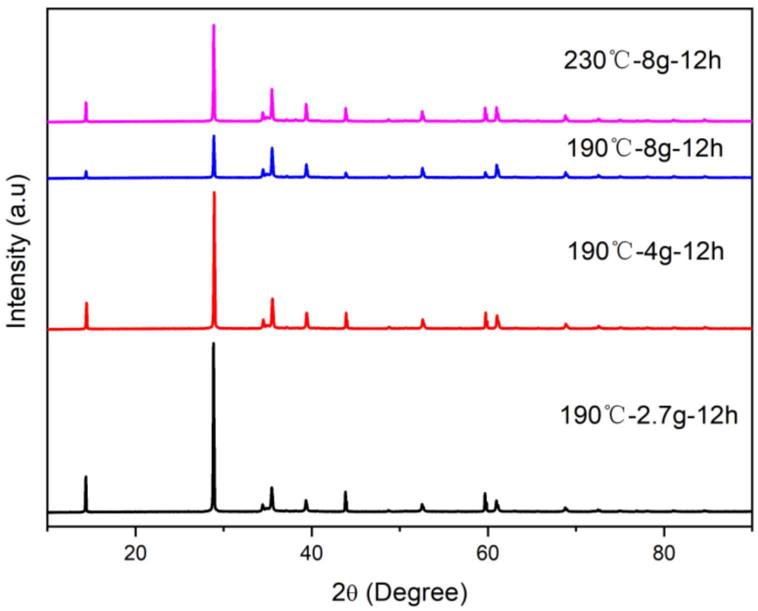

Figure S10. XRD patterns; (b-e) SEM of $AgFeO_2$ nanosheets regulated by different (001) polar surfaces.

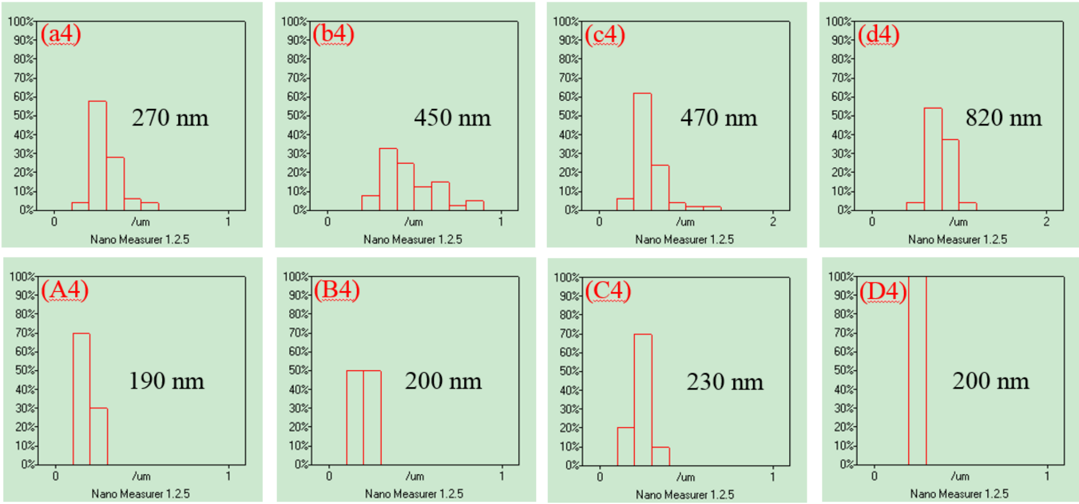

Figure S11. (a4-d4) width and (A4-D4) thickness of $AgFeO_2$ nanosheets with different (001) polar exposed surfaces.

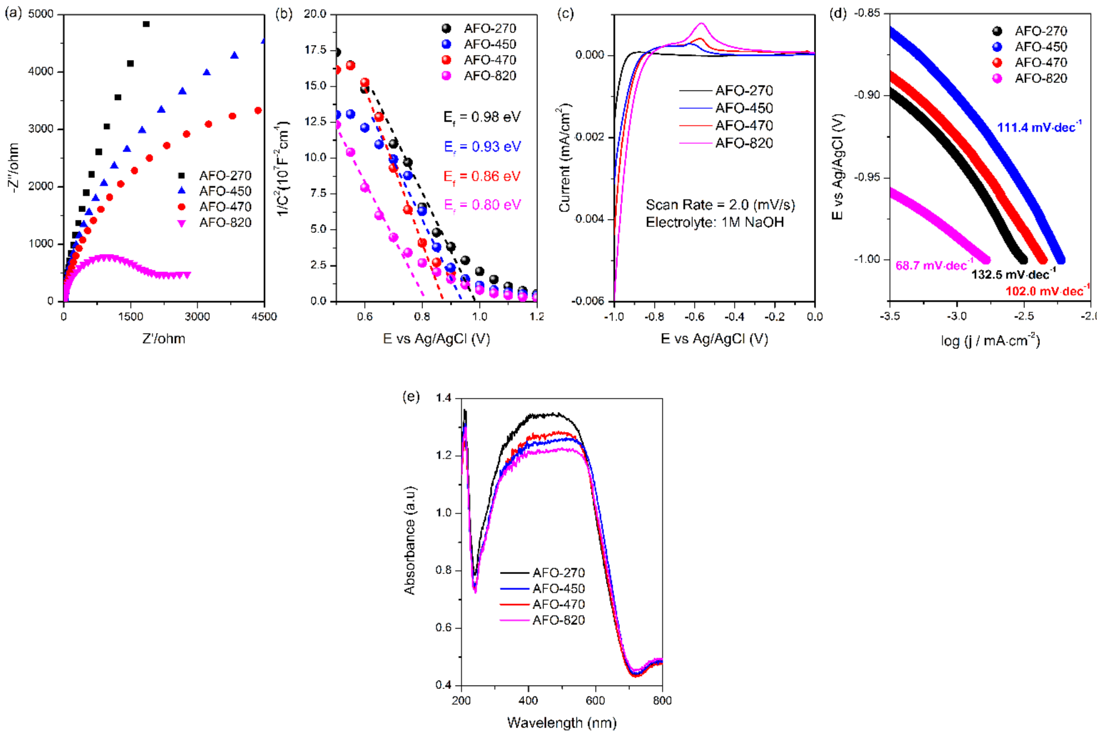

Figure S12. (a) EIS curves; (b) M-S curve; (c) the LSV curve; (d) Tafel slope diagram; (e) UV-Vis curve of $AgFeO_2$ electrodes with different (001) polarity exposure surfaces.

Table S1. The regulation of hydrothermal reaction temperature, time and NaOH concentration on the size of $AgFeO_2$ nanosheets.

Reaction temperature	Reaction time	NaOH concentration	Nanosheet width	Nanosheet thickness	Crystalline phase	Sample labeling
190℃	12 h	1.5 g (1.875 mol/L)	-	-	No pure phase is formed	-
190℃	12 h	1.8 g (2.250 mol/L)	-	-	No pure phase is formed	-
190℃	12 h	2.1 g (2.625 mol/L)	100 nm	40 nm	3R	AFO-100
190℃	12 h	2.7 g (3.375 mol/L)	270 nm	190 nm	3R	AFO-270
190℃	12 h	4.0 g (5.000 mol/L)	470 nm	230 nm	3R	AFO-470
190℃	12 h	8.0 g (10.00 mol/L)	450 nm	200 nm	3R	AFO-450
180℃	12 h	2.4 g (3.000 mol/L)	-	-	No pure phase is formed	
190℃	12 h	2.4 g (3.000 mol/L)	250 nm	180 nm	3R	AFO-250
210℃	12 h	2.4 g (3.000 mol/L)	280 nm	220 nm	3R	AFO-280
230℃	12 h	2.4 g (3.000 mol/L)	320 nm	250 nm	3R	AFO-320
190℃	6 h	2.1 g (2.625 mol/L)	-	-	No pure phase is formed	
190℃	9 h	2.1 g (2.625 mol/L)	-	-	No pure phase is formed	
190℃	15 h	2.1 g (2.625 mol/L)	380 nm	210 nm	3R	AFO-380
190℃	24 h	2.1 g (2.625 mol/L)	540 nm	270 nm	2H, 3R	AFO-540
190℃	48 h	2.1 g (2.625 mol/L)	-	-	No pure phase is formed	
210℃	12 h	2.7 g (3.375 mol/L)	300 nm	140 nm	3R	AFO-300
230℃	12 h	8.0 g (10.00 mol/L)	820 nm	200 nm	3R	AFO-820
230℃	48 h	8.0 g (10.00 mol/L)	1000 nm	350 nm	3R	AFO-1000

Table S2. The BET area and electrochemically active surface area (ECSA) of typical $AgFeO_2$ nanosheets.

Characteristics	Label	Thickness (nm)	BET area (m^2/g)	$\frac{\text{BET area}}{\text{Thickness}}$	Normalized ECSA (cm^2)	$\frac{\text{ECSA}}{\text{Thickness}}$
Comparable exposed area	AFO-100	40	3.8246	0.0956	0.7412	0.0185
	AFO-300	140	5.4547	0.0390	0.7456	0.0053
	AFO-820	200	6.9024	0.0345	0.7450	0.0038
	AFO-470	230	6.5179	0.0283	0.7432	0.0032
	AFO-1000	350	4.7389	0.0135	0.9729	0.0028
Comparable thickness	AFO-820	200	6.9024	0.0345	0.7450	0.0038
	AFO-470	230	6.5179	0.0283	0.7432	0.0032
	AFO-450	200	5.6059	0.0280	0.6295	0.0031
	AFO-270	190	3.6666	0.0193	0.5673	0.0030